The deformation and displacement simulation of clay slope are shown in Fig.5 and Fig.6. In order to be observed clearly, the model is divided into grids with different colors. The results of sand slope simulation can be seen in Fig.7 and Fig.8.

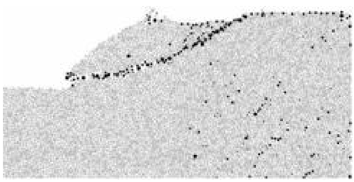

Fig. 9. Diagram of rotation grades of particles

Fig. 10. Diagram of particles direction angle

In displacement diagrams, fracture of sand slope exhibits suddenness.

Fig.9 shows rotation grades of particles. In the diagram the dark color denotes that the rotation angle is larger than 10 degrees. As seen in Fig.9, the particle rotation only occurs within the shear band and most sliding particles keep rigid movement.

The particle angle in Fig.10 has been partially magnified, in which the lines direction represent the angle of each particle. Except the particles in shear band, the directions of the rest particles remain unchanged and keep horizontal. And particles on top of the slope are dense, while the porosity of particles at the bottom becomes larger obviously. The evolution of porosity in different location is shown in Fig.11. At the beginning, the compression of the particles lead to the emergence of shear band and the dilation of material which results in the porosity increasing at the bottom and in the middle of soil slope. When shear band links up, the particles moves and then re-arranges under loading. Finally, the equilibrium condition is reached through the adjustment of the particles inter-force and the sliding surface comes into being as well.

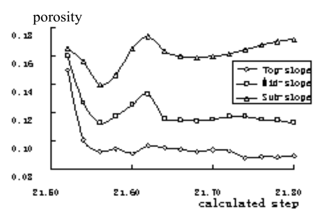

Fig.11. Evolution of porosity

EFFECTS OF MESO-MECHANICS PARAMETERS ON SLOPE FAILURE FORM

It is well-known that slope failure form is influenced by internal structure and external conditions. This paper investigates the effects of meso-mechanics parameters of particle, including linkage strength and friction coefficient. Parameters of PFC model are shown in Table 3.

In Fig.12, linkage strength of particles is zero, which means the soil is non-cohesive and the linkage of particles lies in contact stress completely. Initial failure occurs from the top of the slope, which causes large-scale sliding due to the loss of the support of the top and the middle of the slope. For the clay case, the initial failure occurs at the top of the slope at the beginning, and cracks can be detected from the slope surface. And then at the middle of the slope larger cracks turn out which cause the shear slide. Finally the entire slope slides along the failure surface.

Table 3. Parameters of model PFC

Particle model	Linkage strength (Pa)	Friction coefficient	Density (kg/m^3)	Kn(Pa)	Ks(Pa)
Model-1	0	0.9	2600	6e8	6e8
Model-2	1e5	0.9	2600	6e8	6e8
Model-3	3e5	0.9	2600	6e8	6e8
Model-4	3e5	0.5	2600	6e8	6e8

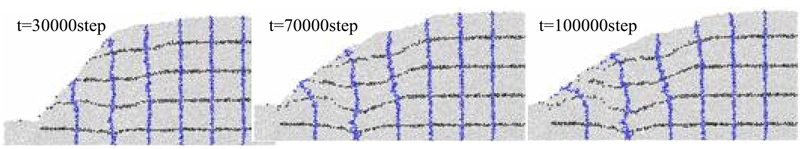

Fig.12. Process of slope failure (pb=0, f=0.9)

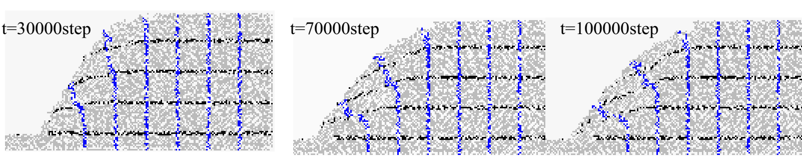

Fig.13. Process of slope failure ($pb = 100kpa, f = 0.9$)

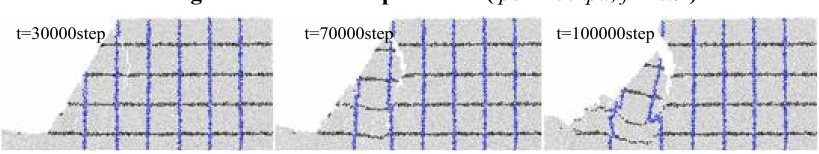

Fig.14. Process of slope failure ($pb = 300kPa, f = 0.9$)

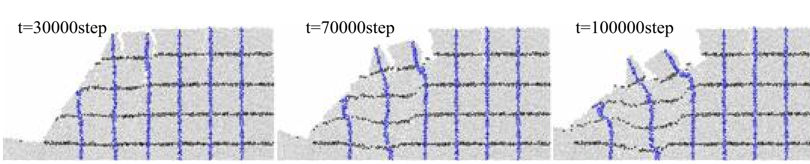

Fig. 15. Process of slope failure ($pb = 300kPa, f = 0.5$)

Therefore, slope deformation and failure form are influenced by meso-parameters. With the increasing of clay cohesion, slope fracture changes from plastic failure to brittle failure. For non-cohesive slope, the entire slope body presents a plastic flow state, without any obvious cracks.

CONCLUSIONS

Based on the theory of particle flow, the development of displacement field of the sliding slope is simulated without assuming the location and shape of sliding surface, which overcomes the deficiency of macro-continuity assumption in continuum mechanics and is more logical than conventional search method for locating the critical sliding surface. From the displacement field of particles and emergence and development of shear band, it can be concluded that the results of the simulation generally satisfy the test results.

The results of the research help to comprehend mechanical characteristics of soil and the process of successive failure of slope. In future research, we will improve the precision of the results by using three-dimensional approach to simulate the slope deformation.

ACKNOWLEDGMENTS

Funding for this work was provided by The National Natural Foundation of China (50178054).

REFERENCES

Cundall,P.A.(1989).“Numerical Experiments on Localization in Frictional Material.” *Ingenieur-Archiv*, Vol .59:148-159.

JIANG Minjing and SHENG Zhujiang.(1998). “Microscopic analysis of shear band in structured clay.” *Chinese J. of Geotechnical Eng.*, 20(2):102-108

Oda,M. and Kazama,H. (1998). “Microstructure of shear bands and its relation to the mechanism of dilatancy and failure of dense granularsoils.” *Geotechnique*, Vol48(4):465-481

Khalid,A and Alshibli,S. S. (1999). “Sand shear band thickness measurement by digital imaging techniques.” *J. of Computing in Civil Eng.*, 13(2):103-109

White,D. J. and Take,W.A.(2002). “A deformation measurement system for geotechnical testing based on digital imaging,close-range photogrammetry and PIV image analysis.” 15th ICSME, Rotterdam: Balkema :539-542.

ZHOU Jian, et al. (2000). “The method of particle flow and PFC2D code.” *Rock and Soil Mechanics*.Vol.21(3):271–274.

BARDET,J P and PROUBET,J.(1991). “A numerical investigation ofstructure of persistent shear bands in granular media.” G*eotechnique*, 41(4):599–613.

MUHLHAUS,H.B. and VARDOULAKIS,I. (1987). “The thickness of shearbands in granular materials.” *Geotechnique*,Vol.37:271–283.

ZHOU Jian, et al. (2000). “Simulation of biaxial test on sand by particle flow code.” *Chinese J. of Geotechnical Engineering*, .22(6):701–704.

Bardet,J.P. and Proubet,J. (1991). “A numerical investigation of structure of persistent shear bands in granular media.” *Geotechnique*, 41(4):599-613.

ZENG Yuan. (2006). “Microscopic Mechanics of Soil Failure and PFC Numerical Simulation.” *PhD dissertation, Tongji University*.

Influence of Soil Strength on Reinforced Slope Stability and Failure Modes

Hong-Wei Wei[1], Ze-Hong Yu[1], Jian-Hua Zhang[2], Zhi-Hui Zhu[1], and Xiao-Li Yang[1]

[1]Professor,School of civil and architecture engineering, Central south university, Changsha, China, 410075. E-mail: whw.edu@163.com.
[2]Engineer, Ning-Dao Expressway Development Limited Company, Changsha, China,410075.

ABSTRACT: Finite element method was applied to analyze the reinforced slope stability in the paper, and under conditions of reinforcement materials matched with soil of various strengths, the shear zone characteristics and failure modes, as well as the influences of the soil strength parameters on reinforced effect, were also investigated. Results showed that reinforcement had increased significantly the apparent cohesion of soil, the reinforced sandy slope was damaged along a certain sliding arc, and appeared the cohesive slope destruction characteristics, the failure modes of the traditional sand slopes were varied correspondingly, and the integrity and stability of sandy slopes were all improved. Even with the same reinforcement material, reinforcement effect on the stability of the slope differed with various index of soil strength. The selection of the strength combinations of reinforcement and soil within a certain range could sufficiently mobilize the interactions to improve the reinforcement effect. Results also showed that reinforcement could improve the soil strength and enhance the stability of the slope to a certain extent, but could not change the main body of soil in the reinforced slope. Considering the combination of reinforcement and soil is crucial to ensure the reinforced effect in reinforced slope design.

INTRODUCTION

In the past 10 years of highway construction projects, Application of reinforced embankment slope with geosynthetics had developed very rapidly, Reinforced soil with geosynthetics improved soil strength and the overall stability of the embankment slope, particularly in mountain highway, through rational design of the reinforcement, the height of reinforced slope could increase by 10% to 30% compared with that of soil slops, thus reduced significantly the field occupation and fill construction. Reinforcement technique possesses a good application prospect.

Influence factors on reinforced soil strength are complex, not only depended on the strength of reinforced material, but also on that of the soil, as well as the interaction between soil and reinforcement. For a certain strength of the reinforced material, matched with the soil of different strengths, the interaction characteristics differed, reinforced soil appeared different strength characteristics, the research can be found in the literature of O'Rourke & Druschel (1990), Zou & Zhang (1998), Wei & Yu (2005) et al. As a result, ignorance of the combination of reinforcement and soil in the reinforced slope designs might usually be the key reason to cause failure of reinforced slopes, the related work accidents had been discussed in literature [7].

Influences of reinforcement modulus and layers on shear zone yield characteristics and failure modes of the reinforced slope had been investigated by Yu in 2003-2004, but the impact of soil strength on the stability of reinforced slope might be the same important factor. Finite element analysis models of a reinforced embankment slopes were established and the visual graphics technology was also applied to research reinforced soil slope stability, as well as the shear zone yield characteristics and failure modes with various soil friction angle φ and cohesion c, and its influences on the reinforced effect. In comparisons with test results, the calculation models and analysis results were reasonable.

FINITE ELEMENT METHOD FOR REINFORCED SLOPE STABILITY

The stability of the reinforced slopes was determined by the combination work of soil and reinforcement. Therefore, the plane units, one-dimensional linear units were all set up to simulate soil and reinforcement material respectively, and only the reinforcement axial stress were considered, while the bending stress were ignored in finite element calculation. Between soil and reinforcement the contact friction units were used to simulate their interactions. The slope stability analysis was simplified by plane strain problem in the paper.

In the reinforced slope, reinforced materials and soil went through almost the same strain due to the extensity of Geosynthetics, only when collapse happened in reinforced slope, a relatively small slide emerged, therefore, within a certain range of deformation, soil and reinforced materials deformation were compatible, in order to simplify the calculation, assuming that the node-node contact on two surface, and maintaining a small amount of deflection, contact elements were applied to simulate the state of the work on reinforcement and soil interface. The reinforced materials were laid on all around the whole width of embankment with uniform distribution. The boundary conditions were given as vertical rollers on the left and right boundary, full fixity at the base, and free boundary at the rest .

The Soil model used in this study consists of six parameters: internal angle φ cohesion c, elastic modulus E, Poisson's ratio μ dilatancy angle ψ unit weight γ

The dilatancy angle ψ affects the volume change of soil during yielding , if $\phi=\psi$ then plasticity flow rule is associated, and direct comparison with the classical plasticity theory can be made, but the calculation of dilatancy is too large than that is observed in reality. This in turn leads to increased failure load prediction, especially in confined problems, the constitutive soil models to incorporate non-associated plasticity are used to resolve. Slope stability analysis is relatively unconfined, so the choice of dilation angle is less important. The value $\psi=0$ had been used in the paper, corresponding to a non-associated flow rule with zero volume change during yield. Griffiths (1999) studies showed that this option enabled the model to give reliable factors of safety and reasonable potential failure surface shapes and locations.

Mohr-Coulomb yielding criterion remains widely used in geotechnical practice, but Mohr-Coulomb yielding surface was an irregular hexagonal section with cone angles, brought the numerical difficulties. Broading Mises yield criteria is cone-shaped surface, and can be written as follows:

$$\alpha I_1 + \sqrt{J_2} = k \quad (1)$$

Where: I_1, J_2 are the first invariant of stress tensor and the second invariant of stress tensor deviator. α,κ are constants related with the rock material. In plane π, α,κ represent various circles, and through different transformation of expressions of α,κ, various yielding criterions can be realized in the finite element .In order to compare with the traditional method, Xu, Gan-Cheng, Zheng, Ying-ren (1990) put forward equivalent area with Mohr-Coulomb criterion in place of traditional Mohr-Coulomb yield criterion, the calculation results were close to that with Mohr-Coulomb criterion, compared with Bishop simplified method, the average error of the slope safety factor calculated was 5.7%, and calculation dispersion was smaller. α,κ can be written as follows:

$$\alpha = \frac{2\sqrt{3}\sin\varphi}{\sqrt{2\sqrt{3}\pi\left(9-\sin^2\varphi\right)}} \qquad k = \frac{6\sqrt{3}c\cos\varphi}{\sqrt{2\sqrt{3}\pi\left(9-\sin^2\varphi\right)}} \quad (2)$$

The factor of safety of slope was defined in the paper as the number by which the original shear strength parameters might be divided in order to bring the slope to point of failure. The soil friction angle and cohesion were input, and gravity load were imposed step-by-step during calculation. And then the soil strength parameters c, φ were gradually reduced uptill to the reinforced slope sliding appearance, the factored shear strength parameters c', φ' were just the required strength of soil to remain the equilibrium of slope. The factor of safety of slope was therefore given by:

$$c' = \frac{c}{F_s};\tan\varphi' = \frac{\tan\varphi}{F_s} \quad (3)$$

The stresses and strains were redistributed in reinforced slope, due to the finite element method solutions would give information about the internal stresses and deformations of slope, therefore, the influences of reinforcement force on stresses on the potential sliding surface, and the stabilizing effect of reinforcement were considered more comprehensively.

The shear zone going through was taken as an indicator of failure in the paper. During calculation, slope failure and numerical non-convergence occurred simultaneously, and were accompanied by a dramatic increase in nodal displacements within the mesh, when close to the real safety factor F_s.

INFLUENCES OF SOIL STRENGTH PARAMETERS ON REINFORCED SLOPE STABILITY

In the examples studied, the slope was inclined at an angle of $\beta=40^0$, the height H=20m. Calculation parameters included: unit weight $\gamma=21\text{kN/m}^3$, elastic modulus E=20MPa, Poisson's ratio μ=0.3; tensile modulus of reinforcement E_R=200kN/m, the number of reinforcement layer n=8. Normal rigidity coefficient of interface between soil and reinforcement FKN=1E6kN/m^2, and tangential rigidity coefficient $FKT \leq 320$ kN/m^2.

Effects of cohesion on reinforced slope stability

Given the soil friction angle $\varphi=15^0$ and $\varphi=30^0$, the safety factors of reinforced and unreinforced slopes were all calculated with various cohesion c, the safety factor increments with increasing cohesion c of reinforced slopes in comparison with that of soil slope were summarized in Table1, and illustrated in Fig.1.

For the same reinforcement modulus and layer, the increments of reinforced slopes differed with the various cohesions. Due to the reinforced soil significantly improving the apparent cohesion the safety factor increased larger relatively when the soil cohesions were low. Reinforced effect of the stability were not the same either under different friction angles, in particular, when both the friction angles and cohesion were lower, the safety factor increments of reinforced slopes increased more significantly. Therefore, the main contributions to the slope stability made by reinforcement attributed to the increase of soil cohesion.

Table 1. Safety Factor Increments of Reinforced Slope in Relation to Soil Slope with Various Cohesion *c*

	Cohesion *c*/ kPa									
	120	100	80	60	40	20	10	5	1	0.1
Safety factor increments/%, when φ=30°	5.86	6.51	7.33	9.95	6.59	7.69	9.17	9.18	9.20	9.52
Safety factor increments/%, when φ=15°	3.54	4.17	9.84	8.50	9.02	10.3	8.82	10.5	12.2	14.3

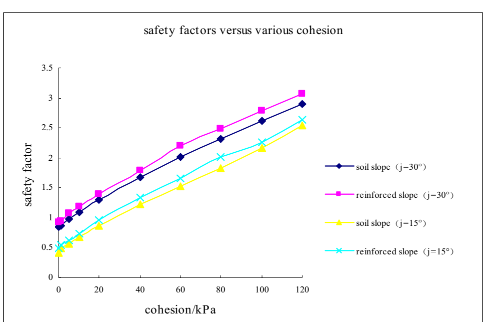

Fig.1. Safety factor of slopes versus cohesion *c*

In the soil slope, safety factor appeared linear increase with the cohesion increase, while in the reinforced slope the safety factor increment varied with the different cohesion c. In the range of cohesion c less than 20kPa, the space of safety factor envelopes of the reinforced slope and soil slope were smaller relatively compared with that of the cohesion in 20kPa ~100kPa, and when cohesions were greater than 100kPa the space tended to be stable. These showed that within cohesion of 20kPa to 100kPa, the interaction between soil and reinforced material appeared coordinating, and reinforced effects on stability safety factor increase were more significant. Taking into account the slope safety factor value in the Norm, in this example, the filling material cohesions should be chosen in range of 20kPa~100kPa.

Effects of cohesion on reinforced slope shear zones and failure modes

The shear zones of soil slope when the cohesion close to c=0 were illustrated in Fig.2 (a). As a result of the limitation of calculation model, c=0.1kPa was used to simulate the soil without cohesion, in this situation, the shear zones calculated of the reinforced slopes were similar with that of sandy slopes, the results at the same time showed the rationality of calculation model.

The reinforced slope shear zones moved towards the internal slopes and foundation as illustrated in Fig.2 (b), the failure modes appeared destruction characteristics of the cohesive slopes, the slope integrity was enhanced, and the tendency to soil cohesion increase was conformed to the test results.

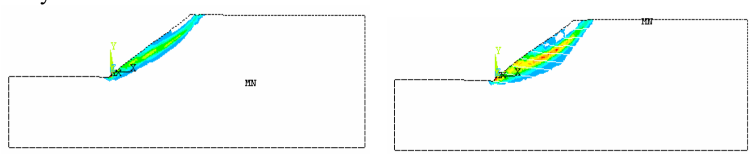

(a) c=0.1kPa, Fs =0.42 (b) c=0.1kPa, Fs =0.48

Fig.2. The shear zones of soil slopes versus various cohesion

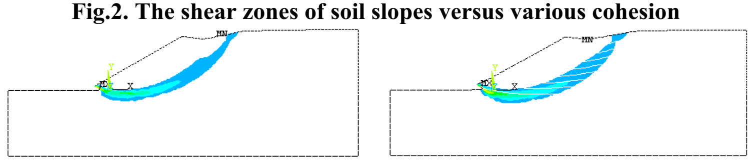

(a) c=100kPa, Fs =2.16 (b) c=100kPa, Fs =2.78

Fig.3 Shear zones of reinforced slopes with various soil cohesion

With the reduction of soil cohesion, the shear zones of both the reinforced and soil slopes moved towards the surfaces of slope, as illustrated in Fig.2 and Fig.3. But the shear zone width of the reinforced slope along the reinforcement direction was wider apparently, and showed more soil near the shear zone was involved in resistance to slope sliding due to the friction and bite between soil and reinforcement, in addition, the tensile strength and separation of reinforcement all prevented the partial damage from the continuity, and enhanced the stability of the slope. At the same time, even if the cohesion c=0.1kPa, the shear zone of reinforced slope still possessed a certain angle with the slope surface, and tended to slip along a certain arc, with a cohensive slope failure feature. The plane failure modes of non-cohesive sand slope had been revised due to reinforcement, as showed in Fig.2 (a) (b).

The cohesion strength of reinforced soil consists of two parts, one was possessed by soil itself, and the other was reinforced by the interaction of reinforcementl and soil. The triaxial test and direct shear test results all showed that the strength increase of reinforced soil mainly caused by the apparent cohesion increase, seen in literature [7-8]. These calculation results not only showed the effects of reinforcement on slope stability differed with various soil cohesion, but also the reinforced slopes differed essentially from the unreinforced in the safety factors, performances of shear zones and failure modes, as illustrated in Fig.2 (a) (b). In particular, when the soil cohesion reduced down to c=0.1kPa, this appeared more intuitively. Therefore, for the sandy slope, reasonable reinforcement enabled slope stability improved, but the failure mode of sliding parallel to the slope surface also varied correspondingly.

Effects of various friction angles φ on reinforced slope stability

In the examples studied, the soil cohesion were given as c=40kPa and 60kPa respectively, other calculation parameters were the same as that above.

Safety factors of reinforced and unreinforced soil slopes were summarized in Table2. The safety factor of slopes were significantly reduced with the soil friction angle reduction, down close to φ=0^0, the safety factors of the reinforced and unreinforced slopes were almost equal, and reinforcement had no action on slope stability, as illustrated in Fig. 4, whether reinforced or soil slope, their safety factors reduced with the friction angle, the decrement of safety factor increased at $\varphi \leq 5^0$.

Table 2. Slope Safety Factors with Various Soil Friction Angles

	Friction Angle φ							
	45°	35°	25°	15°	10°	5°	1°	0°
Soil Slope (c=60kPa)	2.56	2.17	1.85	1.54	1.35	1.15	0.94	0.845
Reinforced Slope(c=60kPa)	2.70	2.38	2.03	1.68	1.46	1.21	0.95	0.854
Safety Factor Increment/%	5.47	9.68	9.73	9.09	8.15	5.23	1.06	1.06
SoilSlope(c=40kPa)	2.25	1.87	1.52	1.22	1.07	0.86	0.65	0.556
Reinforced Slope(c=40kPa)	2.34	1.95	1.66	1.31	1.13	0.92	0.67	0.563
Safety Factor Increment/%	4.00	4.28	9.21	7.38	5.61	6.98	3.08	1.26